ONCOIMMUNOLOGY
2023, VOL. 12, NO. 1, 2203073
https://doi.org/10.1080/2162402X.2023.2203073

Taylor & Francis
Taylor & Francis Group

BRIEF REPORT

OPEN ACCESS Check for updates

Expression of *OLR1* gene on tumor-associated macrophages of head and neck squamous cell carcinoma, and its correlation with clinical outcome

Peng Zhang[a#], Yan Zhao[b#], Xin Xia[c#], Song Mei[d], Yixuan Huang[e], Yingying Zhu[c], Shuting Yu[c], and Xingming Chen[c]

[a]Beijing Key Laboratory for Genetics of Birth Defects, Beijing Pediatric Research Institute; MOE Key Laboratory of Major Diseases in Children; Rare Disease Center, Beijing Children's Hospital, Capital Medical University, National Center for Children's Health, Beijing, China; [b]Department of Otolaryngology Head and Neck Surgery, Beijing Tongren Hospital, Capital Medical University, Beijing, China; [c]Department of Otolaryngology-Head and Neck Surgery, State Key Laboratory of Complex Severe and Rare Diseases, Peking Union Medical College Hospital, Peking Union Medical College and Chinese Academy of Medical Sciences, Beijing, China; [d]Shanghai Institute of Immunology, Shanghai Jiao Tong University School of Medicine, Shanghai, China; [e]Division of Immunotherapy, Institute of Human Virology, University of Maryland School of Medicine, Baltimore, MD, USA

ABSTRACT

Head and neck squamous cell carcinoma (HNSCC) is one of the most heavily immune infiltrated human tumors, having distinct immune subtypes associated with different molecular characteristics and clinical outcomes. The tumor microenvironment (TME) of HNSCC which was dominated by tumor-associated macrophages (TAMs) had a relatively inferior prognosis. High levels of oxidized low-density lipoprotein receptor 1 (*OLR1*) expression are associated with more aggressive and metastatic characteristics in multiple cancers. However, the link between the *OLR1* expression and immunosuppression of TME, and the molecular mechanisms which govern intratumoral TAMs behavior are unclear. Here, we performed the transcriptional analysis based on a single-cell RNA-sequencing (scRNA-seq) dataset of HNSCC, and found that the *OLR1* expression was specifically enriched on the TAMs. Evaluation of protein expression within histologic sections of primary HNSCC patient samples showed a co-expression pattern of *OLR1* and *CD68* on macrophages. A total of 498 tumor samples of HNSCC patients from The Cancer Genome Atlas (TCGA) database were also analyzed. Remarkably, *OLR1* expression was dramatically higher in HNSCC tissues than that in adjacent normal tissues, and the patients with high levels of *OLR1* expression had significantly unfavorable overall survival (Hazard Ratio = 1.724, log-rank *P*-value = 0.0066) when compared to patients harboring low expression levels of *OLR1*. In summary, we reported that the specific expression of *OLR1* on the TAMs was significantly correlated with poor survival outcomes, revealing that *OLR1* could serve as a potential prognosis marker and promising target for immunotherapy in HNSCC.

ARTICLE HISTORY
Received 8 February 2021
Revised 24 March 2023
Accepted 10 April 2023

KEYWORDS
scRNA-seq; HNSCC; OLR1; Macrophage; Biomarker

Introduction

Tumor-associated macrophages reside within the tumor microenvironment in head and neck squamous cell carcinoma and generally correlate with poorer outcomes[1,2]. *OLR1* is a lectin-like scavenger receptor that could recognize several ligands, such as oxidized low-density lipoprotein (LDL)[3]. The overexpression of *OLR1* was reported to be associated with the upregulation of several oncogenes and the promotion of cell apoptosis, proliferation, and migration in various cancer types[4]. Interestingly, recent studies[5] showed that the LDL was one of the most increased regulators and its receptor *OLR1* was one of the most overexpressed genes in polymorphonuclear myeloid-derived suppressor cells (PMN-MDSC).

Previous studies demonstrated that TAMs were increased in the TME of HNSCC, and the samples with a higher abundance of TAMs showed correlated immunosuppressive effects[6]. TAMs in HNSCC can also produce significant levels of macrophage migration inhibitory factor, which is an inflammatory cytokine that stimulates the invasiveness of the tumor cells[7,8]. Therefore, TAMs may represent a therapeutic target for the HNSCC, and there are multiple clinical assessments of specific agents targeting TAMs under development[9]. Here we performed our analysis to address whether the *OLR1* gene has the potential to be a transcriptional marker of TAMs behavior in the tumor microenvironment and a prognosis marker for the overall survival of HNSCC patients. Our study supports the utilization of *OLR1* expression by macrophages to predict patient outcomes, which may have important implications for future clinical use as a prognosis marker or potential immunotherapy treatment target for HNSCC.

CONTACT Peng Zhang zhangpengdyx@163.com Beijing Key Laboratory for Genetics of Birth Defects, Beijing Pediatric Research Institute; MOE Key Laboratory of Major Diseases in Children; Rare Disease Center, Beijing Children's Hospital, Capital Medical University, National Center for Children's Health, Beijing 100045, China; Xingming Chen xingming.chen@hotmail.com Department of Otolaryngology-Head and Neck Surgery, State Key Laboratory of Complex Severe and Rare Diseases, Peking Union Medical College Hospital, Peking Union Medical College and Chinese Academy of Medical Sciences, Beijing 100005, China
[#]Contribution equally.

Supplemental data for this article can be accessed online at https://doi.org/10.1080/2162402X.2023.2203073

Materials and methods

Single-cell sequencing data analysis

The scRNA-seq dataset of head and neck cancer samples was accessed from NCBI's Gene Expression Omnibus database (http://www.ncbi.nlm.nih.gov/geo/) through accession number: GSE103322 and GSE139324. Analyses were then performed using R software (https://www.r-project.org/, version 4.0) and primarily using the package "Seurat". To process data, cells were filtered, and a total of 4,541 cells were kept based on the filtering criteria: 1) the number of genes detected per cell>300 and<4000, and 2) the percent of mitochondrial genes<0.10. Expression profiles were log-normalized and scaled whereby the percent of mitochondrial genes was regressed out. Clusters were determined by using the first 15 principal components and graphed by using the Uniform Manifold Approximation and Projection (UMAP) dimensional reduction method for each sample. The identified cell clusters that, through conventional marker genes, could be readily assigned to known cell lineages. The TAMs derived from GSE139324 were redone normalization, scaling, and clustering by UMAP processes and annotated by canonical markers (*C1QA*, *SPP1*, *INHBA*, *NLRP3*, *CLEC5A*, and *HSPA1B*).

TCGA patient cohort

The molecular data and clinical annotation from cancer patient samples (HNSCC, 498 samples) were obtained from public repositories based upon data generated by TCGA Research Network (http://cancergenome.nih.gov/). The clinical data (including overall survival status and time) of cancer samples were accessed from the cBioPortal for Cancer Genomics database (http://www.cbioportal.org/index.do, February 2020). The mRNA expression quantification (HTSEQ-FPKM) profiles based on the RNA-sequencing were downloaded from the TCGA data portal (https://portal.gdc.cancer.gov/, February 2020). We use the information integrity based on the clinical annotation and bulk RNA-seq expression profiles of the TCGA database to select the HNSCC patients in this study. Only the cancer patients with available and complete prognostic annotation and RNA-seq profiles will be kept for downstream analysis.

Human HNSCC specimens

Patients at the Peking Union Medical College Hospital (PUMCH) consented preoperatively to take part in the study following Institutional Review Board approval (Protocol #S-K795). HNSCC patients with newly diagnosed, histopathologically confirmed, untreated patients were consecutively recruited at PUMCH from July 2019 to December 2019. Written informed consent was obtained from all patients enrolled in this study. All lesions were classified according to the histological typing criteria of the World Health Organization (WHO). The clinical information of human subjects providing samples is listed in **Table S1**.

Immunohistochemistry (IHC) staining

Sectioning and IHC staining were performed based on the formalin-fixed, paraffin-embedded (FFPE) HNSCC specimens and their paired normal mucosae. All sections were 4 μm thick. Antigen retrieval was achieved by heating in citrate acid (pH 6.0) using a programmable microwave. Then, sections were treated with freshly prepared 3% hydrogen peroxide in methanol for 20 min and further washed in Tris-buffered saline. The continuous sections were incubated with *OLR1* antibody (diluted 1:100, rabbit polyclonal) (Proteintech, Chicago, Illinois, USA; 11837–1-AP) and *CD68* antibody (diluted 1:1000, mouse monoclonal) (Abcam, Cambridge, MA, USA; ab233172) at 4°C overnight, respectively. After the tissues had been rinsed three times with PBS for 5 min, a two-step IHC detection kit (Servicebio, Wuhan, Hubei, China, G1210–2) was used. Primary antibodies were visualized with horseradish peroxidase-linked (HRP-linked) secondary antibodies, and then followed by diaminobenzidine (DAB) according to the manufacturer's instructions. The staining sections were observed under a light microscope. The staining of tissue was scanned using Pannoramic Desk Scanner (3DHistech, Budapest, Hungary) at 20× and viewed using CaseViewer software (Version 2.3).

Immunofluorescence (IF) staining

FFPE HNSCC specimens and their paired normal mucosae were performed to 4 μm thick sections. IF staining was performed according to standard staining methods, including deparaffinization and rehydration, endogenous peroxidase quenching, and then heat-mediated antigen retrieval with citrate acid (pH 6.0) and blocking with blocking buffer (3% BSA and 0.2% Triton in PBS). The section was incubated with both *OLR1* antibody (diluted 1:200, rabbit polyclonal) (Sino Biological, Beijing, China; 10585-T26) and *CD68* antibody (diluted 1:50, mouse monoclonal) (Abcam, Cambridge, MA, USA; ab233172) at 4°C overnight. After rinsing, the sections were incubated with Alexa Fluor 568 Anti-Rabbit IgG (diluted 1:1000) and Alexa Fluor 488 Anti-Mouse IgG (diluted 1:1000) for 1 h at room temperature and counterstained with 4,6-diamidino-2-phenylindole dihydrochloride (Sigma-Arich, #D952) for the staining of nuclei. After washing with PBS, the coverslips were mounted with antifade mounting medium (Beyotime, Shanghai, China) on slides. The staining of tissue was scanned using Pannoramic Desk Scanner (3DHistech, Budapest, Hungary) at 40×, and viewed using CaseViewer software (Version 2.3).

Flow cytometry

Rinse the HNSCC tissue in a dish containing PBS to remove erythrocytes and cut the tissue into pieces. Transfer a maximum of 1 g cancer tissue to a gentleMACS C Tube containing 5 mL enzyme mix according to the manufacturer's instructions of the human Tumor Dissociation Kit (Miltenyi Biotec, Cologne, Gemany; 130-095-929). Single cells were resuspended with FACS buffer (calcium and magnesium-free PBS supplemented with 0.1% BSA) and stained with FITC-

conjugated anti-human mAbs against *OLR1* (Abcam, Cambridge, MA, USA; ab81710) and AF647-conjugated anti-human mAbs against *CD68* (Thermo Fisher, 51-0689-42) and isotype-matched IgG for 30 min at 4°C, after preincubation with rabbit IgG to block nonspecific sites. Fluorescence was quantitated on an Agilent NovoCyte 3005 flow cytometer equipped with NovoExpress Software (Agilent). Cells were gated according to their light-scatter properties to exclude cell debris.

Quantification and statistical analysis

The specific tests used to analyze each set of experiments are indicated in the figure legends. For the comparison of the quantitative data between two different groups, the Mann-Whitney test was used to calculate the *P*-value. For the analysis of the contingency tables, Fisher's exact test was used to calculate the significance. To perform a patient's cohort-based analysis on the overall survival rate (5-year), the prognostic value of discrete variables was estimated by using the Kaplan-Meier survival curves, and the log-rank test was employed to estimate the significance among different survival curves. All statistical calculations were performed using GraphPad Prism software (GraphPad Software, version 8.0, San Diego, California) or R software (version 4.0, https://www.r-project.org/).

Results

Firstly, to determine whether *OLR1* expression is associated with TAMs infiltration, transcriptional analysis based on a publicly accessible scRNA-seq dataset[10] of HNSCC samples was initially performed. After quality control filtering to remove cells with low gene number detection and high mitochondrial gene coverage, a unified cells-by-genes expression matrix of a total of 4,541 single cells from 17 head and neck squamous cell carcinoma (HNSCC) patients was compiled. As shown in Figure 1A, the 12 major cell phenotypes were identified by using the unsupervised dimensionality reduction and visualized by the Uniform Manifold Approximation and Projection (UMAP) algorithm. The canonical marker genes for each cell lineage were applied to annotate the clusters (Figure 1B). We investigated the expression distribution of *OLR1* across different cell types and found that it was specifically enriched on the tumor-associated macrophages ($N = 97$) when compared with other cell types (P-value<0.0001) (Figure 1C). Besides, a recently published work of an available scRNA-seq dataset[11] with more abundant immune cell profiled based on the TME of HNSCC was also included for the validation of our findings based on scRNA-seq expression profiles (**Figure S1**). A total of 3930 TAMs were clustered into 6 different subtypes, which respectively expressed *C1QA*, *SPP1*, *INHBA*, *NLRP3*, *CLEC5A*, and *HSPA1B* (Figure 1D & 1E). All these TAM subtypes expressed *OLR1*, among which Macro_INHBA and Macro_NLRP3 showed a higher expression level (Figure 1F).

Next, to confirm the expression pattern of *OLR1* on TAMs of the TME in HNSCC, we co-stained primary HNSCC samples and paired normal mucosae from 9 HNSCC patients (including three different sub-types) with *OLR1* and *CD68* to detect the protein expression of *OLR1* by macrophages. As expected, *OLR1* staining was highly specific and localized to the CD68+ TAMs across different stages and various subtypes of HNSCC samples, while *OLR1* and *CD68* were in an extremely low expression level in their paired normal mucosae tissues (Figure 2A). In addition, immunofluorescence staining (Figure S2) and flow cytometric (Figure S3) analysis were also performed to confirm the localization of *OLR1* on the macrophages. The clinical characteristics of the 9 HNSCC patients who had primary HNSCC within our cohort are summarized in **Supp Table 1**. Then, a total of 498 tumor samples of HNSCC patients with transcriptional data and clinical annotation based on the largest publicly available cancer-genomic studies TCGA database were also involved in this work. The bulk RNA-sequencing data were analyzed using five different algorithms (CIBERSORT[12], XCELL[13], EPIC[14], TIMER[15], and MCPCOUNTER[16]) to estimate the intratumoral macrophage infiltration, respectively. Remarkably, we found that all the estimated abundance of macrophages based on different methods were significantly positively correlated with the expression of *OLR1* transcripts (Figure 2B). Collectively, the transcriptional analysis and protein staining results revealed the *OLR1* specifically expressed on TAMs of the TME in HNCSS, and its expression value could serve as an indicator for macrophage infiltration.

Then, we determined the correlation of expression of the *OLR1* gene with clinical characteristics in HNSCC samples from TCGA. The results revealed the transcripts of *OLR1* were dramatically enhanced in paired HNSCC samples ($N = 42$) compared with adjacent normal tissues (P-value = 0.0007) (Figure 3A). The same trend was also observed when comparing the estimated macrophages abundance between paired HNSCC samples and adjacent normal tissues (P-value = 0.0092) (Figure 3B). Interestingly, we found a weak association between high *OLR1* expression value and advanced clinical stage (Figure 3C) in this data set. There is no difference in *OLR1* expression between HPV+ and HPV- status was overserved (Figure 3D). Besides, we also compared the expression of *OLR1* with other risk factors (including alcohol consumption and smoking) of HNSCC, and as shown in Fig.S4, there is no association between *OLR1* expression value and alcohol consumption and smoking status. Moreover, we systematically analyzed the clinical data of patient cohorts to evaluate the prognosis function of different features by using univariate cox regression analysis, and the results showed the *OLR1* gene expression value exhibited a meaningful predictor for the clinical outcome of HNSCC patients (Figure 3E). The patients with low levels of *OLR1* expression had significantly better overall survival than those with low *OLR1* expression (Hazard Ratio = 1.724, log-rank P-value = 0.0066). And it is worth noting that when combining the survival comparisons with *OLR1* expression and estimated

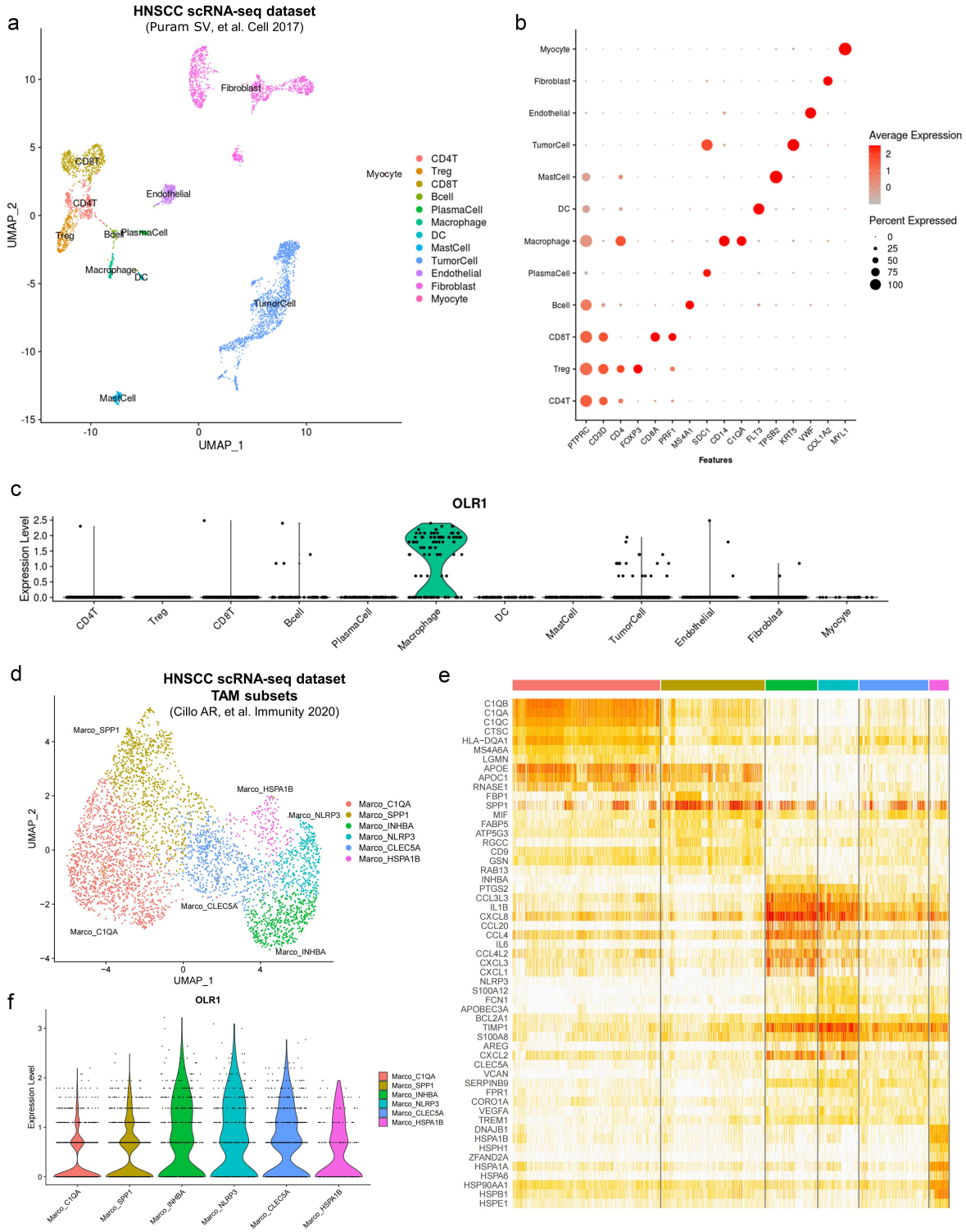

Figure 1. scRNA-seq analysis revealed *OLR1* specifically expressed on tumor-associated macrophages. (A) Uniform Manifold Approximation and Projection (UMAP) plots of the scRNA-seq dataset from HNSCC samples. Infiltrating phenotypic cell clusters are represented in distinct colors. (B) Dot-plot of expression distribution of canonical markers for each cell type identification. (C) Violin-plot displaying the expression patterns of the *OLR1* gene within each cell type. (D) UMAP plots of TAMs from a distinct scRNA-seq dataset. Different TAM subsets are represented in distinct colors. (E) Heatmap of top 10 highly expressed genes in each TAM subsets. (F) Violin-plot displaying the expression level of the *OLR1* gene in the different TAM subsets.

TAM infiltration abundance, the HNSCC patients with low levels of both macrophage infiltration and *OLR1* expression had superior survival compared with other subgroups of patients (Figure 3E). In addition, to determine the general significance of the association between *OLR1* expression and cancer prognosis, we also analyzed the other eight common cancer types (including BLCA: Bladder urothelial carcinoma; BRCA: Breast invasive carcinoma; COAD: Colon adenocarcinoma; KIRC: Kidney renal clear cell carcinoma; LUSC: Lung squamous cell carcinoma; OV: Ovarian serous cystadenocarcinoma; UCEC: Uterine corpus endometrial carcinoma; STAD: Stomach adenocarcinoma)

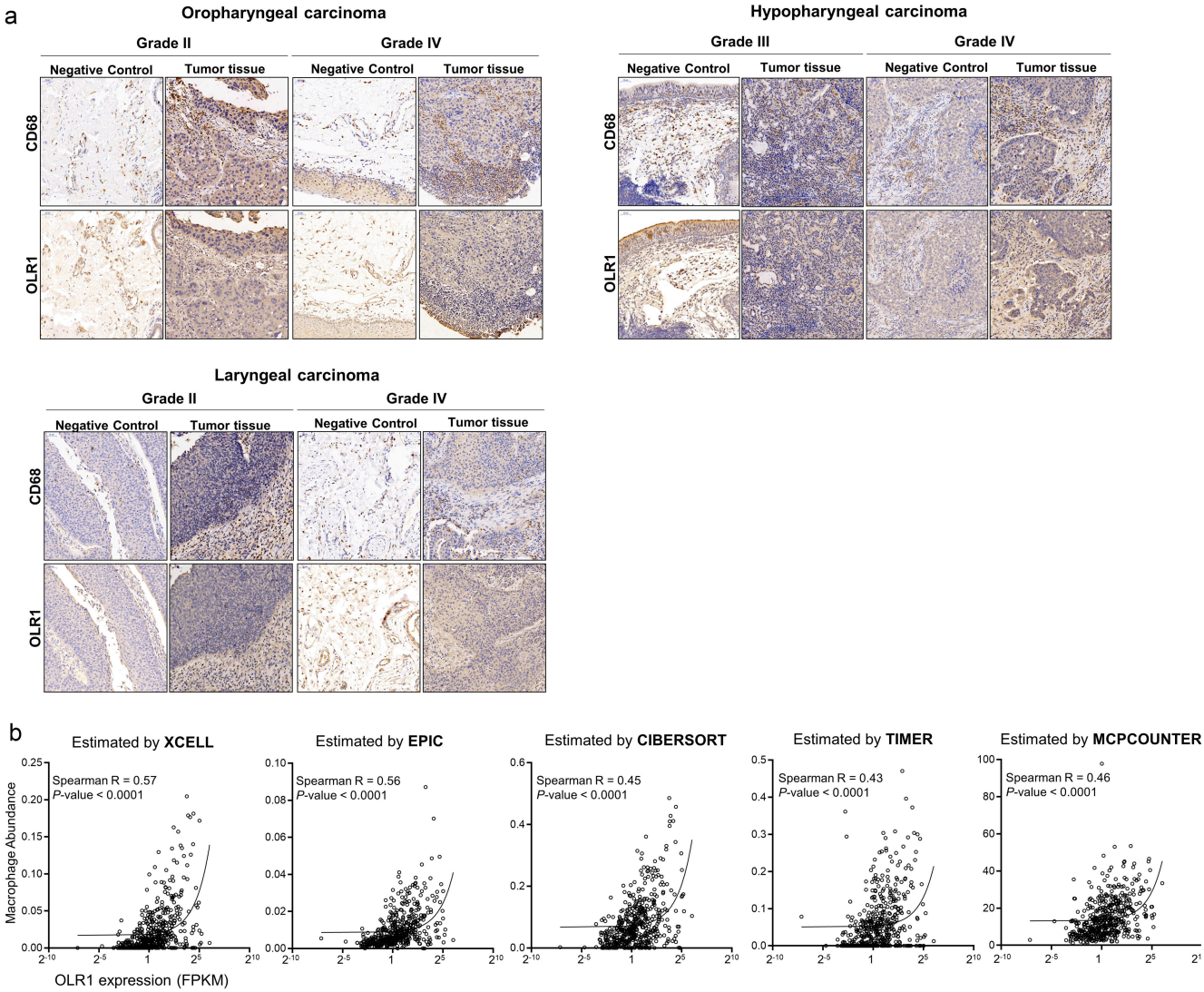

Figure 2. Correlation of intratumoral *OLR1* expression and macrophage infiltration. (A) Immunohistochemistry staining analysis of *OLR1* and *CD68* in HNSCC tumor samples. (B) Correlation of estimated tumor-associated macrophage abundances by using different methods and *OLR1* expression value based on TCGA database.

to define the pan-cancer prognosis value of *OLR1* expression. As shown in **Figure S5**, although a similar trend was observed in all other cancer cohorts based on the TCGA database, none of the tumor types could achieve a significant prognosis threshold, so we conclude that the prognosis significance *OLR1* is HNSCC cancer type specific.

Discussion

Previous studies on *OLR1* mainly focused on its roles in cancer development, such as tumorigenesis, cancer development, and metastasis. For example, activation of the TNFα/NF-κB pathway or PI3K/Akt/GSK3β pathway could upregulate *OLR1* to facilitate the migration and metastasis of breast cancer and gastric cancer cells, respectively[17–19]. However, the current understanding of the underlying mechanism of the oncogenesis function of *OLR1* in the tumor microenvironment remains limited. HNSCC develops within a complex cellular environment that includes many different types of infiltrating immune cells, which could promote tumor growth but also represent potential therapeutic targets[20,21]. The presence of TAM within the tumor microenvironment has been implicated in the growth, aggression, and persistence of HNSCC. And the numerous present findings revealed the prognostic significance of the phenotypes and abundances of TAMs, and indicated variable degrees of association between TAMs density and clinicopathologic features of HNSCC. However, the current methods that evaluating TAMs in the TME have occasionally been contradictory that result in the high TAMs levels could both negatively and positively correlate with the outcome, signifying that the specific behavior markers of TAMs rather than the quantity of the infiltrate are a more reliable indicator. We also investigate the expression correlation between *OLR1* and macrophage polarization markers (such as *CD163* and *HLA-DR*) based on the HNSCC patient cohort of TCGA, and the

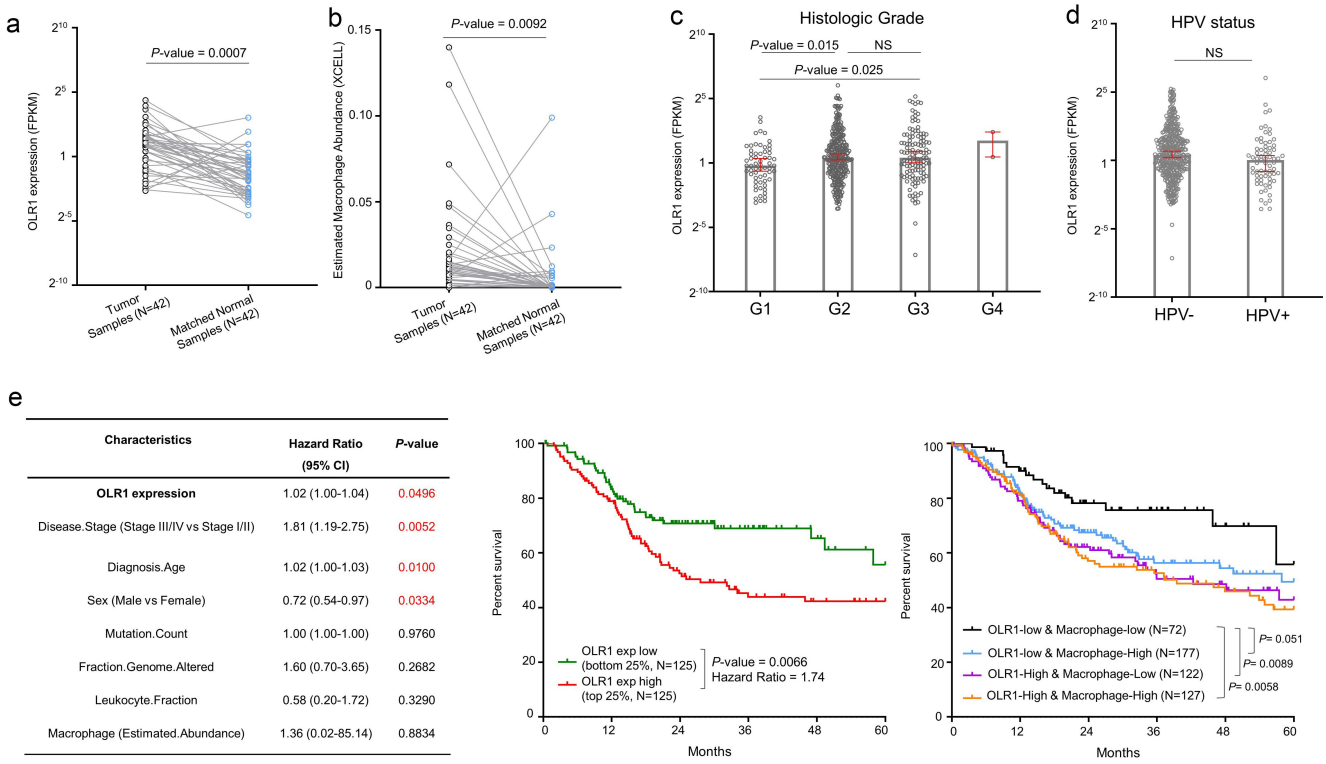

Figure 3. Higher intratumoral *OLR1* expression levels were associated with worse survival. (A) Change of *OLR1* mRNA expression between matched tumor and normal samples ($N = 42$). (B) Change of estimated macrophage abundance between matched tumor and normal samples ($N = 42$). (C) The distribution plot of *OLR1* gene expression among different disease stages. (D) The distribution plot of *OLR1* gene expression among HNSCC patients with different HPV statuses. (E) The univariate cox regression analysis table (left) and Kaplan-Meier plot (right) show the *OLR1* gene expression correlated with worse overall survival (5-year) of the TCGA HNSCC cohort. The *P*-value in A and B was determined by the Paired t-test. The *P*-value in C was determined by the One-way ANOVA. The *P*-value in D was determined by the Mann-Whitney test. The *P*-value and Hazard Ratio in E were determined by the log-rank test.

results revealed a strong positive association between *OLR1* and *CD163* (**Figure S6**), indicating the *OLR1* may contribute to recapitulating M2-polarized TAMs in the TME of HNSCC. So, since one of the major aims of current immunotherapy approaches is to target the tumor microenvironment to promote an anti-tumor response of the surrounding immune cells and *OLR1* might be an interesting target.

Here, we propose that *OLR1* could be a mechanical link between tumor immunosuppression and cancer progression, and we conducted an integrative study to evaluate the prevalence of *OLR1* expression in the tumor microenvironment and its correlation with TAMs abundance and clinical characteristics in HNSCC. Our results evaluated the expression of the *OLR1* gene by TAMs and provided the first evidence that it could be used to predict the inferior survival of HNSCC patients. Further investigations in a larger cohort of HNSCC patients are needed to determine its potential as an ideal candidate prognosis marker and tailor optimal immunotherapeutic strategies for clinical use.

Author contributions

P.Z. Y.Z. and X.X. performed the analysis and prepared the manuscript with the help of Y.H., M.S., Y.Z., and S.Y.; P.Z. and X.C. supervised the studies, designed the analysis, and revised the manuscript.

Availability of data or materials

The materials of patient cohorts used for the current study were publicly available and can be assessed by the TCGA database (https://portal.gdc.cancer.gov/). The scRNA-seq datasets of head and neck cancer samples could be accessed from NCBI's Gene Expression Omnibus database (http://www.ncbi.nlm.nih.gov/geo/) through accession number: GSE103322, and GSE139324. The processed data and analysis codes are available upon reasonable request from the corresponding author.

Disclosure statement

No potential conflict of interest was reported by the authors.

Funding

This work was supported by the National Natural Science Foundation of China (81273173 and 82000962), Chinese Academy of Medical Sciences (CAMS) Innovation Fund for Medical Sciences (CIFMS) (2021-I2M-1-023 and 2020-I2M-2-009), Science & Technology Fundamental Resources Investigation Program (2022FY100800), National High Level Hospital Clinical Research Funding (2022-PUMCH-B-094), Beijing Hospitals Authority (QML20211205), Beijing Nova Program (Z211100002121044), and the State Key Laboratory Special Fund (2060204).

ORCID

Peng Zhang http://orcid.org/0000-0002-6218-1885

Ethics approval and consent to participate

This study was approved by the Institutional Review Board (IRB) of the Peking Union Medical College Hospital (PUMCH) (#S-K795). Patients at the PUMCH consented preoperatively to take part in the study following IRB approval and written informed consent was obtained from all patients enrolled in this study. The age and gender of the human subjects providing samples are listed in Table S1.

References

1. Ferris RL. Immunology and immunotherapy of head and neck cancer. J Clin Oncol off J Am Soc Clin Oncol. 2015;33 (29):3293–3304. doi:10.1200/JCO.2015.61.1509.
2. Li B, Cui Y, Nambiar DK, Sunwoo JB, Li R. The immune subtypes and landscape of squamous cell carcinoma. Clin Cancer Res. 2019;25(12):3528–3537. doi:10.1158/1078-0432.CCR-18-4085.
3. Khaidakov M, Mitra S, Kang B-Y, Wang X, Kadlubar S, Novelli G, Raj V, Winters M, Carter WC, Mehta JL. Oxidized LDL receptor 1 (OLR1) as a possible link between obesity, dyslipidemia and cancer. Plos One. 2011;6(5):e20277. doi:10.1371/journal.pone.0020277.
4. Yang G, Xiong G, Feng M, Zhao F, Qiu J, Liu Y, Cao Z, Wang H, Yang J, You L, et al. OLR1 promotes pancreatic cancer metastasis via increased c-myc expression and transcription of HMGA2. Mol Cancer Res. 2020;18(5):685–697. doi:10.1158/1541-7786.MCR-19-0718.
5. Condamine T, Dominguez GA, Youn J-I, V KA, Mony S, Alicea-Torres K, Tcyganov E, Hashimoto A, Nefedova Y, Lin C, et al. Lectin-type oxidized LDL receptor-1 distinguishes population of human polymorphonuclear myeloid-derived suppressor cells in cancer patients. Sci Immunol. 2016;1(2). doi:10.1126/sciimmunol.aaf8943
6. Costa NL, Valadares MC, Souza PPC, Mendonça EF, Oliveira JC, Silva TA, Batista AC. Tumor-associated macrophages and the profile of inflammatory cytokines in oral squamous cell carcinoma. Oral Oncol. 2013;49(3):216–223. doi:10.1016/j.oraloncology.2012.09.012.
7. Dumitru CA, Gholaman H, Trellakis S, Bruderek K, Dominas N, Gu X, Bankfalvi A, Whiteside TL, Lang S, Brandau S. Tumor-derived macrophage migration inhibitory factor modulates the biology of head and neck cancer cells via neutrophil activation. Int J Cancer. 2011;129(4):859–869. doi:10.1002/ijc.25991.
8. Curry JM, Sprandio J, Cognetti D, Luginbuhl A, Bar-Ad V, Pribitkin E, Tuluc M. Tumor microenvironment in head and neck squamous cell carcinoma. Semin Oncol. 2014;41 (2):217–234. doi:10.1053/j.seminoncol.2014.03.003.
9. Mantovani A, Marchesi F, Malesci A, Laghi L, Allavena P. Tumour-associated macrophages as treatment targets in oncology. Nat Rev Clin Oncol. 2017;14(7):399–416. doi:10.1038/nrclinonc.2016.217.
10. V PS, Tirosh I, Parikh AS, Patel AP, Yizhak K, Gillespie S, Rodman C, Luo CL, Mroz EA, Emerick KS, et al. Single-cell transcriptomic analysis of primary and metastatic tumor ecosystems in head and neck cancer. Cell. 2017;171(7):1611–1624.e24. doi:10.1016/j.cell.2017.10.044.
11. Cillo AR, Kürten CHL, Tabib T, Qi Z, Onkar S, Wang T, Liu A, Duvvuri U, Kim S, Soose RJ, et al. Immune landscape of viral- and carcinogen-driven head and neck cancer. Immunity. 2020;52 (1):183–199.e9. doi:10.1016/j.immuni.2019.11.014.
12. Newman AM, Liu CL, Green MR, Gentles AJ, Feng W, Xu Y, Hoang CD, Diehn M, Alizadeh AA. Robust enumeration of cell subsets from tissue expression profiles. Nat Methods. 2015;12 (5):453–457. doi:10.1038/nmeth.3337.
13. Aran D, Hu Z, AJ B. xCell: digitally portraying the tissue cellular heterogeneity landscape. Genome Biol. 2017;18(1):220. doi:10.1186/s13059-017-1349-1.
14. Racle J, Gfeller D. EPIC: a tool to estimate the proportions of different cell types from bulk gene expression data. Methods Mol Biol. 2020;2120:233–248. doi:10.1007/978-1-0716-0327-7_17.
15. Li T, Fan J, Wang B, Traugh N, Chen Q, Liu JS, Li B, XS L. TIMER: a web server for comprehensive analysis of tumor-infiltrating immune cells. Cancer Res. 2017;77(21):e108–110. doi:10.1158/0008-5472.CAN-17-0307.
16. Becht E, Giraldo NA, Lacroix L, Buttard B, Elarouci N, Petitprez F, Selves J, Laurent-Puig P, Sautès-Fridman C, Fridman WH, et al. Estimating the population abundance of tissue-infiltrating immune and stromal cell populations using gene expression. Genome Biol. 2016;17(1):218. doi:10.1186/s13059-016-1070-5.
17. Hirsch HA, Iliopoulos D, Joshi A, Zhang Y, Jaeger SA, Bulyk M, Tsichlis PN, Shirley Liu X, Struhl K. A transcriptional signature and common gene networks link cancer with lipid metabolism and diverse human diseases. Cancer Cell. 2010;17(4):348–361. doi:10.1016/j.ccr.2010.01.022.
18. Liang M, Zhang P, Fu J. Up-regulation of LOX-1 expression by TNF-alpha promotes trans-endothelial migration of MDA-MB-231 breast cancer cells. Cancer Lett. 2007;258(1):31–37. doi:10.1016/j.canlet.2007.08.003.
19. Li C, Zhang J, Wu H, Li L, Yang C, Song S, Peng P, Shao M, Zhang M, Zhao J, et al. Lectin-like oxidized low-density lipoprotein receptor-1 facilitates metastasis of gastric cancer through driving epithelial-mesenchymal transition and PI3K/Akt/GSK3β activation. Sci Rep. 2017;7:45275. doi:10.1038/srep45275.
20. De Felice F, de Vincentiis M, Valentini V, Musio D, Mezi S, Lo Mele L, Terenzi V, D'Aguanno V, Cassoni A, Di Brino M, et al. Follow-up program in head and neck cancer. Crit Rev Oncol Hematol. 2017;113:151–155. doi:10.1016/j.critrevonc.2017.03.012.
21. De Felice F, Polimeni A, Valentini V, Brugnoletti O, Cassoni A, Greco A, de Vincentiis M, Tombolini V. Radiotherapy controversies and prospective in head and neck cancer: a literature-based critical review. Neoplasia. 2018;20(3):227–232. doi:10.1016/j.neo.2018.01.002.